

Dear Author

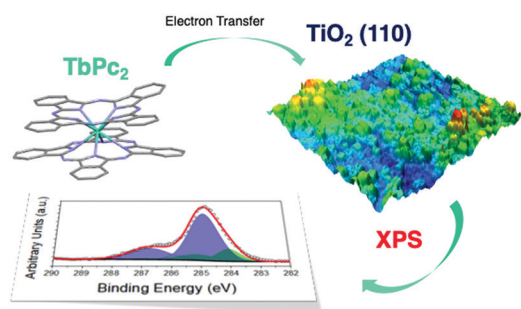
Please use this PDF proof to check the layout of your article. If you would like any changes to be made to the layout, you can leave instructions in the online proofing interface. First, return to the online proofing interface by clicking "Edit" at the top page, then insert a Comment in the relevant location. Making your changes directly in the online proofing interface is the quickest, easiest way to correct and submit your proof.

Please note that changes made to the article in the online proofing interface will be added to the article before publication, but are not reflected in this PDF proof.

If you would prefer to submit your corrections by annotating the PDF proof, please download and submit an annotatable PDF proof by clicking the link below.

 [Annotate PDF](#)

We have presented the graphical abstract image and text for your article below. This briefly summarises your work, and will be presented with your article online.



Substrate mediated interaction of terbium(III) double-deckers with the TiO₂(110) surface

Giulia Serrano,* Andrea Luigi Sorrentino, Lorenzo Poggini,* Brunetto Cortigiani, Claudio Goletti, Roberta Sessoli and Matteo Mannini

STM and XPS characterization studies were used to deeply investigate the chemical environment of TbPc₂ molecules on the TiO₂ rutile surface, probing a strong interfacial interaction independently from surface preparation.

Please check this proof carefully. Our staff will not read it in detail after you have returned it.

Please send your corrections either as a copy of the proof PDF with electronic notes attached or as a list of corrections. **Do not edit the text within the PDF or send a revised manuscript** as we will not be able to apply your corrections. Corrections at this stage should be minor and not involve extensive changes.

Proof corrections must be returned as a single set of corrections, approved by all co-authors. No further corrections can be made after you have submitted your proof corrections as we will publish your article online as soon as possible after they are received.

Please ensure that:

- The spelling and format of all author names and affiliations are checked carefully. You can check how we have identified the authors' first and last names in the researcher information table on the next page. **Names will be indexed and cited as shown on the proof, so these must be correct.**
- Any funding bodies have been acknowledged appropriately and included both in the paper and in the funder information table on the next page.
- All of the editor's queries are answered.
- Any necessary attachments, such as updated images or ESI files, are provided.

Translation errors can occur during conversion to typesetting systems so you need to read the whole proof. In particular please check tables, equations, numerical data, figures and graphics, and references carefully.

Please return your **final** corrections, where possible within **48 hours** of receipt following the instructions in the proof notification email. If you require more time, please notify us by email to pccp@rsc.org.

Funding information

Providing accurate funding information will enable us to help you comply with your funders' reporting mandates. Clear acknowledgement of funder support is an important consideration in funding evaluation and can increase your chances of securing funding in the future.

We work closely with Crossref to make your research discoverable through the Funding Data search tool (<http://search.crossref.org/funding>). Funding Data provides a reliable way to track the impact of the work that funders support. Accurate funder information will also help us (i) identify articles that are mandated to be deposited in **PubMed Central (PMC)** and deposit these on your behalf, and (ii) identify articles funded as part of the **CHORUS** initiative and display the Accepted Manuscript on our web site after an embargo period of 12 months.

Further information can be found on our webpage (<http://rsc.li/funding-info>).

What we do with funding information

We have combined the information you gave us on submission with the information in your acknowledgements. This will help ensure the funding information is as complete as possible and matches funders listed in the Crossref Funder Registry.

If a funding organisation you included in your acknowledgements or on submission of your article is not currently listed in the registry it will not appear in the table on this page. We can only deposit data if funders are already listed in the Crossref Funder Registry, but we will pass all funding information on to Crossref so that additional funders can be included in future.

Please check your funding information

The table below contains the information we will share with Crossref so that your article can be found *via* the Funding Data search tool. **Please check that the funder names and grant numbers in the table are correct and indicate if any changes are necessary to the Acknowledgements text.**

Funder name	Funder's main country of origin	Funder ID (for RSC use only)	Award/grant number
Regione Toscana	Italy	501100009888	POR CreO FESR 2014-2020- SENSOR
European Cooperation in Science and Technology	European Union	501100000921	CA15128 MOLSPIN, Femtoterabyte project
Ministero dell'Istruzione, dell'Università e della Ricerca	Italy	501100003407	B96C1700020008

Q1

Researcher information

Please check that the researcher information in the table below is correct, including the spelling and formatting of all author names, and that the authors' first, middle and last names have been correctly identified. **Names will be indexed and cited as shown on the proof, so these must be correct.**

If any authors have ORCID or ResearcherID details that are not listed below, please provide these with your proof corrections. Please ensure that the ORCID and ResearcherID details listed below have been assigned to the correct author. Authors should have their own unique ORCID iD and should not use another researcher's, as errors will delay publication.

Please also update your account on our online [manuscript submission system](#) to add your ORCID details, which will then be automatically included in all future submissions. See [here](#) for step-by-step instructions and more information on author identifiers.

First (given) and middle name(s)	Last (family) name(s)	ResearcherID	ORCID iD
Giulia	Serrano		0000-0001-7953-7780
Andrea Luigi	Sorrentino		0000-0002-9476-4583
Lorenzo	Poggini		0000-0002-1931-5841
Brunetto	Cortigiani		
Claudio	Goletti		
Roberta	Sessoli		0000-0003-3783-2700
Matteo	Mannini		0000-0001-7549-2124

Queries for the attention of the authors

Journal: PCCP

Paper: **d1cp00928a**

Title: **Substrate mediated interaction of terbium(III) double-deckers with the TiO₂(110) surface**

For your information: You can cite this article before you receive notification of the page numbers by using the following format: (authors), Phys. Chem. Chem. Phys., (year), DOI: 10.1039/d1cp00928a.

Editor's queries are marked on your proof like this **Q1**, **Q2**, etc. and for your convenience line numbers are indicated like this 5, 10, 15, ...

Please ensure that all queries are answered when returning your proof corrections so that publication of your article is not delayed.

Query reference	Query	Remarks
Q1	Funder details have been incorporated in the funder table using information provided in the article text. Please check that the funder information in the table is correct.	
Q2	Have all of the author names been spelled and formatted correctly? Names will be indexed and cited as shown on the proof, so these must be correct. No late corrections can be made.	
Q3	The sentence beginning "The charge transfer processes were also..." has been altered for clarity. Please check that the meaning is correct.	
Q4	The sentence beginning "The shoulder at a lower binding energy..." has been altered for clarity. Please check that the meaning is correct.	
Q5	The sentence beginning "We found that molecular oxidation..." has been altered for clarity. Please check that the meaning is correct.	
Q6	Have all of the funders of your work been fully and accurately acknowledged?	

Substrate mediated interaction of terbium(III) double-deckers with the TiO₂(110) surface†

Cite this: DOI: 10.1039/d1cp00928a

 Giulia Serrano,^{id}*^{ab} Andrea Luigi Sorrentino,^{id}^{ab} Lorenzo Poggini,^{id}*^{ac} Brunetto Cortigiani,^a Claudio Goletti,^d Roberta Sessoli^{id}^a and Matteo Mannini^{id}^a

A terbium(III)-bis(phthalocyaninato) neutral complex was deposited on the rutile TiO₂(110) surface, and their interaction was studied by Scanning Tunneling Microscopy (STM) and X-ray Photoelectron Spectroscopy (XPS). It was found that the TiO₂ rutile surface favours the adsorption of isolated molecules adopting a lying down configuration with the phthalocyanine planes tilted by about 30° when they lie in the first layer. The electronic and chemical properties of the molecules on the surface were studied by XPS as a function of the TiO₂(110) substrate preparation. This study evidences that strong molecule–substrate interactions are present and a charge transfer process occurs from the molecule to the surface.

 Received 1st March 2021,
Accepted 1st May 2021

DOI: 10.1039/d1cp00928a

rsc.li/pccp

Introduction

Single-molecule magnets (SMMs) are a peculiar class of molecules characterized by magnetic bistability at low temperature and, therefore, show magnetic hysteresis properties.¹ They hold promise for quantum computations and spintronics.^{2–5} However, their use is strictly related to the interaction with a solid surface that often alters the molecular structure or magnetic properties.^{6–9} Terbium(III)-bis(phthalocyaninato) molecules, hereafter TbPc₂, represent an archetypal single ion magnet – that is, an SMM achieved exploiting only the anisotropy and the crystal field of a mononuclear-based complex – whose structure consists of a Tb^{III} ion sandwiched between two phthalocyanines (Pc) as ligands.^{10–12} The deprotonation of both Pc ligands and an additional unpaired electron delocalized on the two ligands¹³ impart to the molecule a neutral character. The delocalized electron plays a crucial role in the SMM behaviour¹⁴ and is also significantly participating in the strong surface–molecule interaction with metal substrates leading to the appearance of Kondo features.^{15,16} The structural and

magnetic properties of TbPc₂ films were extensively investigated on various metal surfaces, and it was evidenced that surface–molecule interactions, probably interfering on the delocalization of this unpaired electron, cause the quenching of the SMM magnetic properties on metals.^{7,17–21} Recently, thin insulating layers, *e.g.* graphene,^{17,20} or chemisorption strategies, introduction of a molecular spacer (an alkyl chain group),²² were used to reduce this interaction. It was also reported that the interaction of TbPc₂ with silicon substrates can play an additional role in enhancing the SMM properties (*i.e.* an increased hysteresis opening) due to the stabilization of electron-depleted molecular species.²² Furthermore, an even more pronounced hysteresis opening can be obtained by decoupling the SMM deposit from the metal substrates with a magnesium oxide multilayer.^{18,23} Indeed, MgO films are extensively used to investigate the quantum properties of single atoms on surfaces,^{24–26} evidencing the key role of metal oxides in these studies.

Here, we explore the structural and electronic properties of TbPc₂ SMMs adsorbed on a metal oxide of widespread use, namely titanium dioxide, where both the decoupling effect and electron depletion can occur.^{27,28} This material has a high technological significance, thanks to its photocatalytic and electron transport properties of relevance for sensors or photovoltaic applications.^{27–29} The efficiency of the catalytic and transfer electron processes can be tuned by doping agents or creating surface defects as oxygen vacancies (O-vac), causing excess electrons to be distributed on the surface and introducing defect states within the bandgap.²⁷ The interaction of the most stable surface of titanium dioxide, that is the rutile TiO₂(110) surface,²⁷ with phthalocyanine (Pc) systems has been already thoroughly studied. It reveals strong interactions and

^a Department of Chemistry “U. Schiff” and INSTM Research Unit, University of Florence, Via della Lastruccia 3-13, 50019 Sesto Fiorentino (FI), Italy

^b Department of Industrial Engineering and INSTM Research Unit, University of Florence, Via Santa Marta 3, 50139 Florence (FI), Italy.

E-mail: giulia.serrano@unifi.it

^c Institute for Chemistry of Organometallic Compounds (ICCOM-CNR), Via Madonna del Piano, 50019 Sesto Fiorentino (FI), Italy.

E-mail: lpoggini@iccom.cnr.it

^d Dipartimento di Fisica, Università degli Studi di Roma “Tor Vergata”, Via della Ricerca Scientifica 1, 00133, Rome, Italy

† Electronic supplementary information (ESI) available: Additional XPS, STM and LEED characterization of the sample. See DOI: 10.1039/d1cp00928a

1 the charge transfer processes occurring at the surface–molecule
interface.^{30–32} Electron depletion from the highest occupied
molecular orbital of the TiOPc molecules was observed on
TiO₂(110), and this effect was reduced by the use of pyridines
5 as an interlayer between the materials.³³ The charge transfer
processes were also observed for the electron acceptor
Q3 molecular layers like PTCDA (3,4,9,10, perylene tetracarboxylic
dianhydride, C₂₄O₆H₈)^{34,35} or PTCDI (perylene-tetra-carboxylic-
diimide)³⁶ deposited on TiO₂(110). In many cases, O-vacs were
10 found to act as the catalytic sites for molecular dissociation³⁷ or
the preferential adsorption sites favouring the surface–mole-
cule charge transfer processes.³⁸

To investigate the interaction of TbPc₂ SMMs with a titania
substrate, we deposited a TbPc₂ sub-monolayer on the rutile
15 TiO₂(110) surface in Ultra High Vacuum (UHV) and we studied
their chemical and electronic properties by X-ray Photoemission
Spectroscopy (XPS) and Scanning Tunnelling Microscopy (STM)
measurements. To understand the role of surface defects in the
surface–molecule interactions, we tuned the defect amount by
20 preparing TiO₂ surfaces with different procedures: by (i) sputter-
ing and high-temperature annealing in UHV (TiO₂-HT),^{39,40} (ii)
exposing TiO₂-HT to oxygen (TiO₂-HT_{Ox})^{39,40} and (iii) perform-
ing low-temperature annealing after air exposure (TiO₂-LT)⁴⁰
(for full description, see the Experimental Methods).

Experimental methods

TiO₂(110) surface preparations

30 The TiO₂-HT surface was prepared by cycles of Ar sputtering (1.5
keV energy) and annealing at 1000 K in UHV for 60 min and slowly
cooled down to room temperature by 10 K min⁻¹. The surface was
then studied by XPS and STM measurements as reported in the
text. TiO₂-HT_{Ox} was prepared by following the same procedure of
35 TiO₂-HT but, to completely suppress oxygen vacancies on the
surface (see Results and discussion), the surface was exposed to
an oxygen partial pressure of 2×10^{-7} mbar at room temperature
for 15 min afterwards. The TiO₂-LT surface was prepared by
exposing the TiO₂-HT sample to air for several days to recover
40 the TiO₂ stoichiometry. The sample was then placed in UHV and
gently annealed at 570 K for 60 min. The surface was then checked
by XPS and STM measurements. The Au(111) surface, used as a
reference substrate for TbPc₂ deposition, was prepared in UHV by
cycles of Ar sputtering (1.5 keV energy) and annealing at 770 K. All
45 the surfaces were studied by XPS and STM measurements after
preparation. In the TiO₂-HT_{Ox} case, this control was performed
before and after oxygen exposure.

Molecular deposition and experimental setup

50 Molecular deposition was performed in UHV using a home-
built molecular evaporator in which the molecules were con-
tained in a quartz crucible and heated by a tantalum filament.
Molecules were heated to about 683 K, and the TiO₂ substrate
was exposed to a molecular flux after having determined the
55 deposition rate using a quartz microbalance (about 0.4 nm h⁻¹
for all the depositions). Substrates were kept at room

temperature during all the deposition processes. The deposi-
1 tion time was chosen to ensure the deposition of a sub-
monolayer quantity of molecules. The integrity and coverage
of the molecular deposit were first checked on the Au(111)
5 substrate by STM, showing a coverage of about 15% (see text).
Accordingly, similar deposition times were used for the TiO₂
substrates (20 minutes for TiO₂-HT and TiO₂-HT_{Ox}, and 30 min
for TiO₂-LT). The STM characterization was carried out using
an Omicron Variable-Temperature STM in which the sample
10 was cooled down to 30 K by a liquid helium flux to stabilize
molecular deposits. STM images of all clean substrates were
collected at room temperature. XPS analyses were performed
using a micro-focused monochromatic Al K α radiation source,
 $h\nu = 1486.7$ eV, (XR-MF + Focus 600, by SPECS), and a multi-
15 channel detector electron analyser (SPECS Phoibos 150 1DL).
The X-ray monochromatic beam was set at 54.44° with respect
to the analyser. XPS measurements were recorded in normal
emission and using a pass energy of 40 eV. XPS spectra were
analysed using the CasaXPS software and fitted using a Shirley
20 background. Single-peak components were deconvoluted using
a mixed Gaussian and Lorentzian function (70/30). The Spectra
were calibrated using the Ti^{IV} component at 458.5 eV. LEED
images were acquired using Omicron SpectraLEED rear-view
optics.

Results and discussion

30 TiO₂-HT, TiO₂-HT_{Ox}, and TiO₂-LT samples were characterized
by XPS before and after molecular deposition to determine the
chemical environment of the titania surface and evaluate its
interaction with the TbPc₂ sub-monolayer. Fig. 1a shows the
Ti2p XPS core-level spectra of these three UHV-prepared sur-
35 faces before the deposition of TbPc₂.

The most characteristic peak of the XPS spectrum of TiO₂-
HT is found at about 458.5 eV. It comprises the Ti2p_{3/2}
components associated with the Ti^{IV} species in the bulk and
fivefold-coordinated Ti atom (Ti5c) rows and bridging-oxygen
rows, respectively, that are characteristic of the TiO₂(110)-(1 ×
40 1) reconstruction.^{27,39,41} The shoulder at a lower binding energy
(about 456.6 eV) is associated with the Ti2p_{3/2} component of the
Ti^{III} species (see Fig. 1b) that could arise from (i) the sputtering
Q4 and annealing treatment in UHV causing the formation of
surface oxygen vacancies, (ii) the migration of Ti interstitial
45 atoms from the bulk towards the surface, or (iii) the presence of
hydroxyl groups.^{42–45} The percentage of Ti^{III} in the TiO₂-HT
sample is about 3.2% of the total Ti^{III} and Ti^{IV} Ti2p_{3/2} com-
ponents (see Table S1, ESI†). The spin–orbit component of Ti^{IV}
is found at a binding energy of about 5.7 eV above the main
50 components, while that of Ti^{III} is found at 5.2 eV.⁴⁶ Shake-up at
460.3 eV and plasmons at 471.8, 477.5, and 483.6 eV peaks are
also observed in agreement with the literature reports.^{47–49} The
O1s core-level spectrum (Fig. S1, ESI†) of the clean TiO₂-HT
55 surface is characterized by the main component at about 529.7
eV due to the bulk oxygen species, and a small shoulder (at

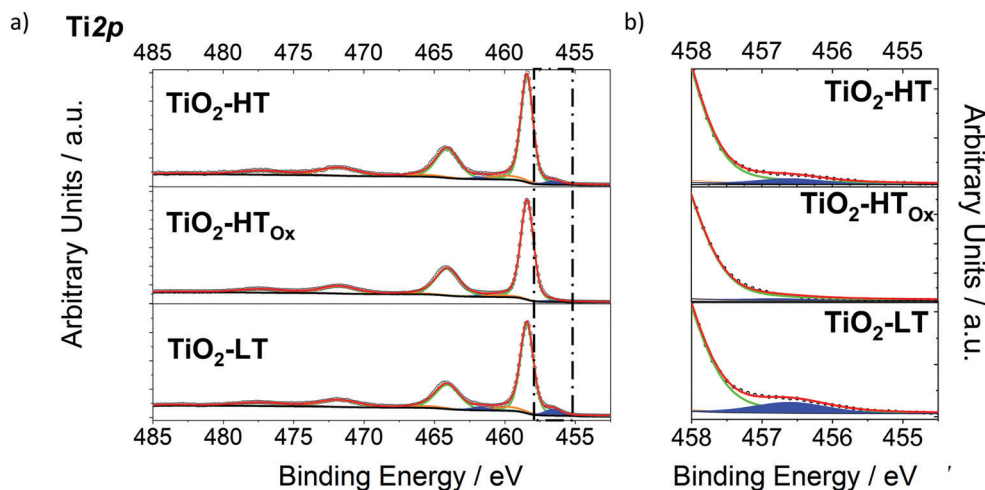


Fig. 1 (a) Ti2p XPS spectra of the TiO₂(110) substrate before molecular deposition for all the three different preparation procedures; (b) zoom in the rectangular region of panel a to emphasise the Ti2p_{3/2} Ti^{III} component obtained from the fitting procedure.

about 530.6 eV) that is attributed to the presence of the Ti^{III} sites and oxygen species (OH groups, water).⁵⁰

The Ti2p and O1s XPS spectra after molecular deposition are reported in Fig. S1, ESI†. We notice that after the deposition of a sub-monolayer of TbPc₂ molecules, the Ti^{III} component of the TiO₂-HT sample is significantly suppressed from 3.4 to 1.7% (see Table S1, ESI†), as observed when molecular species are preferentially bound to the oxygen vacancy sites.³² The high energy component of the O1s signal is only faintly altered by molecular deposition (see Table S1, ESI†). The C1s and N1s core level XPS spectra after TbPc₂ deposition on TiO₂(110) are shown in Fig. 2. The reference spectra of a thick TbPc₂ film (about 14 nm) on Au(111) are shown in the top of Fig. 2 and labelled as TbPc₂ bulk (in the bulk reference spectra, we have omitted the

Tb3d peaks, due to an overlap between this signal and the KLL Carbon Auger peaks⁵¹). The bulk reference C1s spectrum for TbPc₂ is characterized by two main components, one at 284.0 eV corresponding to the benzene carbon species and the second one at 285.2 eV attributed to the pyrrole carbon, and two shake-up components at 286.9 and 287.9 eV. The N1s spectrum of TbPc₂ bulk shows a single component at 398.0 eV and a shake-up component at 399.4 eV. The C1s and N1s contributions of the reference spectra agree with the expected bulk features of phthalocyanines-based compounds,^{32,51–53} thus indicating the integrity of molecules upon thermal sublimation.^{32,52} Interestingly, both N1s and C1s signals are strongly altered when TbPc₂ molecules in the sub-monolayer are in contact with titanium dioxide. On the TiO₂-HT substrate,

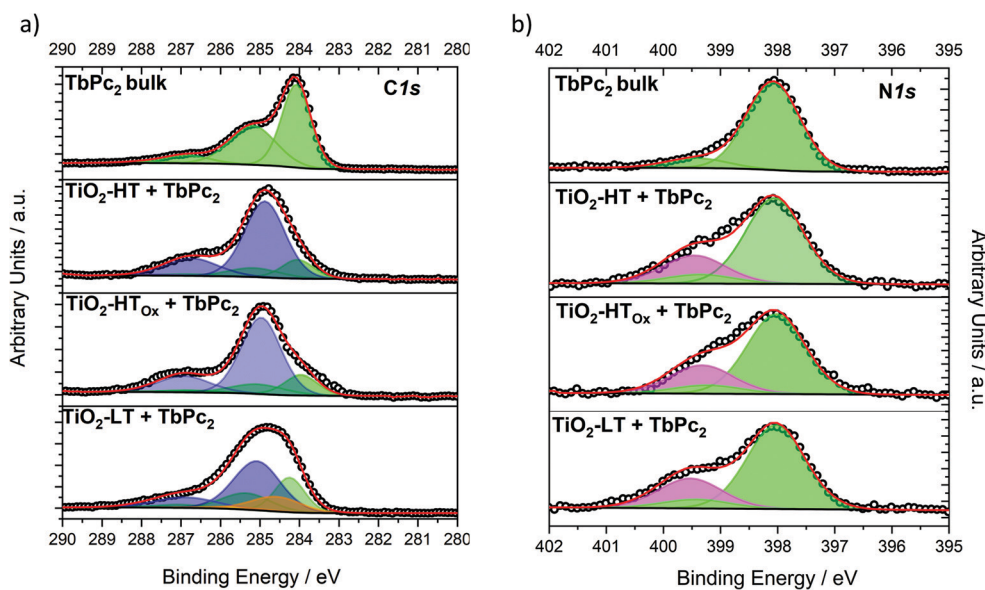


Fig. 2 (a) C1s and (b) N1s core level XPS spectra of a TbPc₂ thick film on Au(111) (TbPc₂ bulk) and TbPc₂ sub-monolayer films on the TiO₂(110) surfaces prepared using different procedures (see text). Bulk-like molecular components are shown in green, while interacting components are shown in blue and pink.

1 the C1s region (Fig. 2a) shows two main peaks around 284.9
and 286.9 eV and a small shoulder around 284.0 eV. The main
features are ascribed to the benzene and pyrrole carbon signals
(blue components) shifted from the bulk ones (green compo-
5 nents) towards higher binding energies of 1.1 and 1.8 eV,
respectively, thus denoting a strong interaction with the sur-
face. Bulk components arise from the shoulder at 284 eV and
are fitted in addition to the interacting components.³² The
coexistence of interacting and bulk-like components was found
10 in the XPS C1s core-level spectrum of metal or free-base
phthalocyanines on TiO₂.^{30–33} The high binding energy compo-
nents were attributed to strong interfacial interactions between
the surface and molecules in the first molecular layer, indicat-
ing that molecules undergo an oxidation process.^{30–33} Interact-
15 ing components were found to vanish with increasing film
thickness, where bulk-like feature dominated.^{30,32} In analogy
with phthalocyanine deposits,^{30–33} also in the present case,
bulk-like components in the C1s spectrum of TbPc₂ on TiO₂-HT
could arise from molecules in the second layer, whose presence
20 is further confirmed by STM experiments reported below.
Besides, the absence of shake-up signals related to the interact-
ing components of the C1s signal (Fig. 2a) suggests an electron
depletion from the molecular layer.^{30–33}

In line with the C1s spectrum, the XPS N1s signal of the
25 TbPc₂ monolayer on TiO₂-HT deviates from the bulk behaviour
(Fig. 2b). The spectrum is characterized by two components, the
first one at 398.1 eV and the second one of a lower intensity at
about 399.4 eV. The low energy component (green) is character-
istic of bulk-like or non-interacting TbPc₂ molecules, while that
30 at 399.5 eV (pink) indicates the presence of oxidized molecular
species, in line with previous observations of Pc species on
TiO₂.^{30–33} or oxidized TbPc₂ complexes grafted on silicon.²²

To clarify whether this interaction arises from the specific
TiO₂ reactive sites, such as O-vac,³⁸ we performed the study on
35 the O-vac-free TiO₂(110) surface (TiO₂-HT_{Ox} sample). O-vac
defect suppression due to oxygen exposure (see Experimental
methods) results in the almost total disappearance of the Ti^{III}
component as evident in the Ti2p XPS spectrum (see Fig. 1
TiO₂-HT_{Ox} and Table S1, ESI†) and the high binding energy
40 (defect-related) component detected in the O1s spectrum (529.8
eV, Fig. S1, ESI†). After TbPc₂ deposition, the XPS C1s and N1s
(TiO₂-HT_{Ox}, Fig. 2) signals look similar to those obtained for
TiO₂-HT, showing no significant variation in energy and intensi-
ty. Furthermore, the Ti2p and O1s signals are not significantly
45 altered by the deposition. These results indicate that the O-vac
sites do not play a central role in the charge transfer process
between the TbPc₂ molecules and the surface. This is at
variance with other molecular compounds, such as 4-*tert*-butyl
pyridine,³⁸ but in line with previous observations on similar
50 systems as the Zn-phthalocyanine films.³² Furthermore, it was
shown by XPS that FePc/FePcF₁₆ deposited on TiO₂ on differ-
ently prepared substrates was not affected by surface
oxidation.⁵⁴ However, in this case, the Pc rings weakly inter-
acted with the substrate.⁵⁴

55 The last TbPc₂ sub-monolayer deposition was carried out on
the TiO₂-LT sample, presenting the most significant deviation

from the expected TiO₂ stoichiometry (see Table S1, ESI†). Here
the Ti2p XPS core level spectrum (Fig. 1) is still dominated by
the Ti2p_{3/2} component of Ti^{IV} but shows a higher intensity of
the Ti^{III} component (7.3% of total signals, see Table S1, ESI†).
The Ti2p shake-up features and the O1s core level spectrum
5 (Fig. S1, ESI†) of the clean TiO₂-LT surface are similar to those
observed in the previous samples. Furthermore, a residual C1s
signal is detected on the surface of the TiO₂-LT sample after
low-temperature annealing (see Fig. S2, ESI†). The C1s region
after molecular deposition (Fig. 2) reveals a complex spectral
10 profile that was fitted using the C1s components of the bulk
TbPc₂ spectrum, the interaction components (two peaks
around 284.9 eV and 286.8 eV), and the additional component
given by the adventitious carbon present on the surface before
molecular deposition. The N1s spectrum of the TbPc₂ sub-
15 monolayer on TiO₂-LT (Fig. 2b) displays two components, in
line with TiO₂-HT and TiO₂-HT_{Ox} (the first one at 398.0 eV and
the second one of lower intensity at 399.5 eV). Therefore, both
C1s and N1s XPS spectra of TbPc₂ on TiO₂-LT confirm the
presence of the interacting components of comparable intensi-
20 ty with respect to the previous samples. From the XPS results,
it is evident that the presence of highly interacting TbPc₂
molecules is independent of the TiO₂ surface preparation
treatment and the presence of the Ti^{III} sites on the surface.
The XPS Tb region was partially covered by the C_{KLL} Auger peak
25 and cannot be used for the semiquantitative analysis or for
understanding the possible involvement of the Tb ion in the
surface interfacial interaction. The FWHM parameters and
peak energy used to fit the C1s and N1s spectra of all samples
are reported in Table S2, ESI.†

STM experiments were performed on the three samples to
investigate the morphological properties of the TiO₂ samples
before and after TbPc₂ sub-monolayer deposition. Fig. 3a
reports an STM image of the clean TiO₂-HT surface. Here bright
and dark rows along the [001] direction are associated with the
35 Ti5c rows and bridging-oxygen rows, respectively, that are
characteristic of the TiO₂(110)-(1 × 1) reconstruction.^{27,39} This
reconstruction was also confirmed by Low Energy Electron
Diffraction (LEED) analysis (see Fig. S3, ESI†). Fig. 3a shows
the presence of point defects, mainly appearing as small bright
40 dots (labelled as type A defects) ascribed to vacant oxygen
atoms in the bridging-oxygen rows. These defects are typically
observed after the high-temperature annealing procedures.^{27,39}
Additional point defects of a greater size, type B, are shown in
Fig. 3a. Line profiles taken across both A and B defects show
45 that they have FWHM values of 0.45 and 0.55 nm, respectively
(see Fig. S4, ESI†). Type A defects show the typical size of O-vac
(FWHM about 0.5 nm from the literature³⁹), while type B
defects could be identified as the hydroxyl groups coming from
water molecule dissociation at the vacancy sites.³⁷ Additionally,
50 the relatively high amount O-vac (type A defects), about 20%
of the surface, indicates the advanced state of the surface
reduction process due to a large number of sputtering and
annealing cycles in UHV. The dark colour of the TiO₂ crystal
and the presence of Ti₂O₃ clusters (marked with an X in Fig. 3a)
55 or strands growing along the [001] direction (see elongated

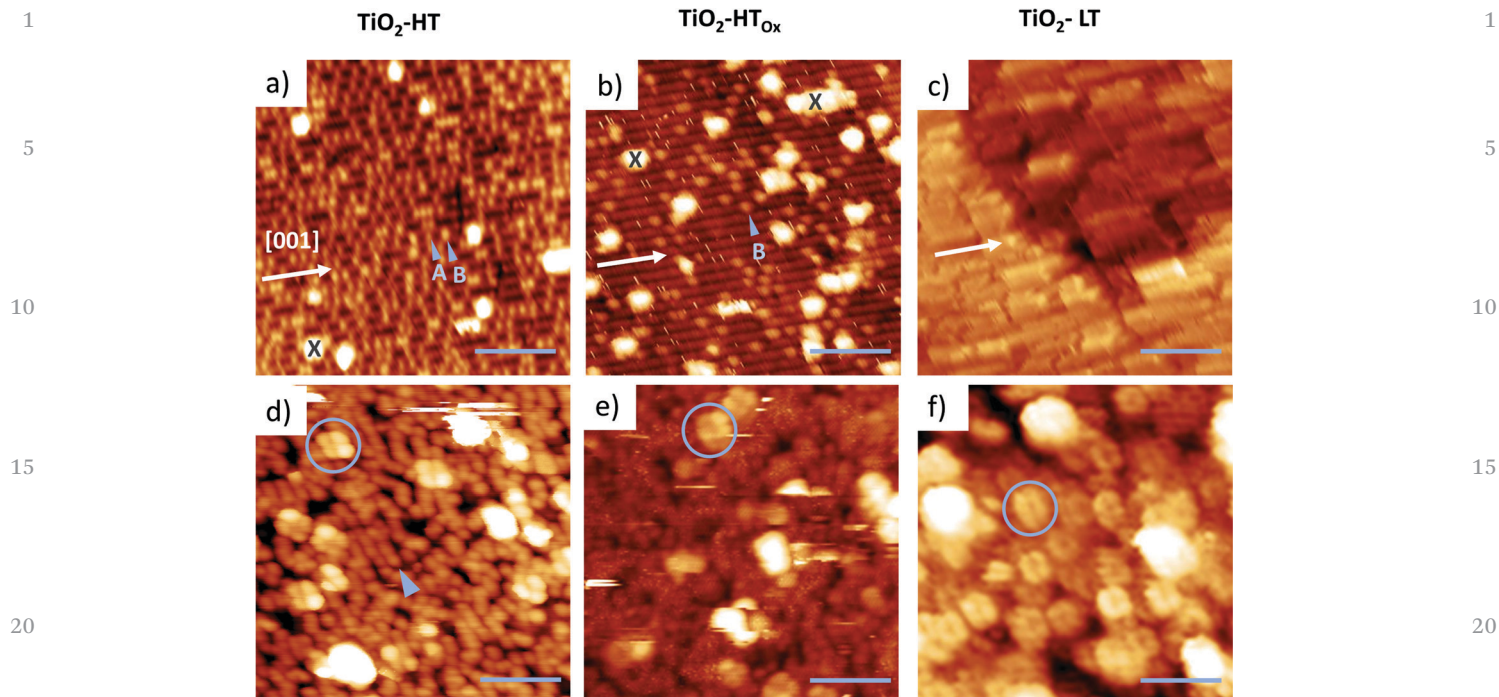


Fig. 3 STM characterization of the $\text{TiO}_2\text{-HT}$, $\text{TiO}_2\text{-HT}_{\text{Ox}}$ and $\text{TiO}_2\text{-LT}$ samples before (a–c) and after (d–f) TbPc_2 deposition, respectively. White arrows indicate the [001] direction. Triangles indicate different point defects on the surface as O-vac sites (A) and OH groups or water molecules (B). Ti_2O_3 clusters or strands are marked with an X (see text). Circles indicate a single molecular unit. STM parameters: (a–c) 2 V, 200 pA; (d–f) 2 V, 3 pA. The scale bar corresponds to 4 nm.

bright features in the Fig. S5a, ESI[†]) are additional pieces of evidence of the advanced reduction state.^{27,55}

Analogous to the $\text{TiO}_2\text{-HT}$ case, the clean $\text{TiO}_2\text{-HT}_{\text{Ox}}$ surface shows Ti and O rows alternating with the same regular periodicity (Fig. 3b). The greater amount of Ti_2O_3 strands (marked with X in Fig. 3b), which is more evident at larger scales (Fig. S6a and c, ESI[†]), is the consequence of the reiterated reduction process in UHV and subsequent exposure to molecular oxygen.^{55,56} In Fig. 3b, no O-vacs are present on the surface as a consequence of the oxygen exposure.³⁹ At variance, small dots in Fig. 3b (type B defects) ascribed to OH groups or water molecules remain on the surface after oxygen exposure (see also line profile in Fig. S6c and d, ESI[†]).³⁷ Instead, the $\text{TiO}_2\text{-LT}$ sample (Fig. 3c) appears to be characterized by a massive presence of Ti_2O_3 strands, while type A and type B defects are no longer evident. However, the greater surface roughness caused by the low-temperature annealing,⁴⁰ hinders the precise characterization of the $\text{TiO}_2(110)$ surface reconstruction on the atomic scale.

Before studying the deposition of TbPc_2 on TiO_2 , molecules were deposited in a sub-monolayer amount on a noble metal substrate, *i.e.* Au(111), to confirm the integrity, purity and dose of the molecular deposit. STM images and line profiles of the molecules on Au(111) (Fig. S7, ESI[†]) indeed show the presence of TbPc_2 molecules covering about 15% of the surface, packed in ordered molecular clusters and having a height of about 0.5 nm, in good agreement with the molecular structure and with previous studies on Au(111).⁵⁷ After depositing a similar TbPc_2 dose on the $\text{TiO}_2\text{-HT}$ surface, the clean substrate's

alternated bright and dark rows are no longer evident (Fig. 3d). However, the comparison of STM images and line profiles before and after deposition (Fig. S5, ESI[†]) confirms that monoatomic steps are still visible as expected from the sub-monolayer molecular coverage. Features with four-lobed shapes in Fig. 3d (circle) are ascribable to the presence of TbPc_2 molecules, similarly appearing on metals^{19,57} or metal oxide surfaces.¹⁸ Surface coverage is around 15%, compatible with that observed on the reference Au(111) surface. STM images reveal that molecules in the first layer adsorb with an inclination of the Pc planes from the surface plane of about $30^\circ \pm 5^\circ$ (see line profiles in the Fig. S8, ESI[†]), causing the different brightness of the four lobes characterizing the single molecular unit. Similar tilting angles could be envisioned for molecules partially sitting on bridging-oxygen sites, as observed for phthalocyanine compounds.⁵⁸ TbPc_2 molecules lie isolated on the surface and adopt a random distribution and orientation at variance with a high-ordered molecular packing found on most surfaces.^{17,57,59} We stress that this is a further indication of a strong interaction with the surface. In contrast, a weak interaction of the molecules on TiO_2 would cause high mobility similar to what was observed by N. Ishida *et al.* for CoPc .⁶⁰ Small bright dots appearing on the surface (indicated by a triangle in Fig. 3d) have dimensions between 0.5 and 0.7 nm (see line profile in the Fig. S8b, ESI[†]) and may be ascribed to H atoms,⁶¹ hydroxyl groups,³⁷ and water molecules^{62–65} in the residual pressure of the evaporation chamber. Their massive presence on the TiO_2 surface at variance with Au(111), although

1 molecular depositions were performed under the same mole- 1
2 cular exposure and residual pressure conditions, can be envi-
3 sioned by taking into account the greater surface reactivity of
4 the titania substrate with respect to noble metals.^{27,61} Further-
5 more, the great affinity of TiO₂ to water molecules has been
6 long studied and debated, showing that water molecules can
7 adsorb or dissociate at O-vac sites.^{61,62,65,66} Fig. S8c in the ESI†
8 shows the TbPc₂ molecules on TiO₂-HT at a larger scale with
9 respect to Fig. 3d and evidences the coexistence of TbPc₂
10 molecules with different heights. By the line profile (Fig. S8d,
11 ESI†), we observe that molecules indicated by empty triangles
12 have a height of *ca.* 0.4 nm and width of about 2.5 nm and
13 therefore could be ascribed to isolated molecules in the second
14 layer.^{31,57} These molecules adopt a perfect lying-down configu-
15 ration with respect to those in direct contact with the surface
16 (filled triangles in the Fig. S8d, ESI†).

17 Despite the increased difficulty in achieving good scanning
18 conditions, single TbPc₂ molecules could be also identified for
19 sub-monolayer deposits on the TiO₂-HT_{Ox} (Fig. 3e, coverage
20 around 10%) and TiO₂-LT (Fig. 3f and Fig. S9, ESI†, coverage
21 40%) surfaces. The higher coverage observed on TiO₂-HT_{Ox} is
22 consistent with the slightly longer deposition time used for the
23 experiment (see Experimental methods) and a possible change
24 of the sticking coefficient with the surface preparation. Further-
25 more, the presence of small dots attributed to the OH groups or
26 water molecules in TiO₂-HT is no longer evident on TiO₂-LT,
27 which could be explained by the higher hydrophobic properties
28 of air-exposed TiO₂ substrates.⁶⁷

29 Finally, the overall STM characterization shows that the
30 different substrate treatments used for TiO₂ preparation induce
31 a similar adsorption configuration and random distribution of
32 the TbPc₂ molecules on the surface.

35 Conclusions

36 We investigated the structural and chemical properties of a
37 sub-monolayer deposit of TbPc₂ molecules on the rutile
38 TiO₂(110) surfaces prepared in UHV by different methods. In
39 particular, we tested three different TiO₂ surface preparations
40 where the annealing temperature and oxygen exposure were
41 varied in order to modify the presence of surface defects, Ti^{III}/
42 Ti^{IV} ratio, as well as sample stoichiometry. The XPS analysis
43 evidenced that all samples are characterized by a strong sur-
44 face–molecule interaction observed in the C1s and N1s spectra
45 of the molecular deposits, strongly differing from the expected
46 bulk-like behavior. The presence of interacting components at a
47 high binding energy points towards an electron transfer from
48 the molecule to the TiO₂ surface. We found that molecular
49 oxidation does neither correlate specifically with the presence
50 of oxygen vacancies on the surface nor with the Ti^{III} content
51 detected by XPS. Still, it is more likely to be dependent on the
52 intrinsic bulk properties of the TiO₂(110) surface as reported for
53 other phthalocyanine-based systems.³² The differences in the
54 surface defects present in the investigated TiO₂ samples do not
55 particularly affect the molecular adsorption configuration

56 observed in the STM images. At variance with other non- 1
57 metal substrates, the lying-down orientation of the Pc molecu- 1
58 lar plane is observed, and molecules lie isolated with a random 1
59 distribution. This tendency to lie isolated could be interesting 1
60 for local STM spectroscopy experiments intended to probe 5
61 single-molecule features.⁶⁸ Additionally, the strong surface- 5
62 molecule interactions detected by XPS are expected to impact 5
63 the electronic and magnetic properties of the molecules. In 5
64 light of the enhanced magnetic bistability observed for TbPc₂ 5
65 on other non-metal substrates and, in particular, on 10
66 MgO,^{17,18,22} the investigation of the magnetic properties of 10
67 the TbPc₂ sub-monolayers on the TiO₂ surfaces by X-ray Mag- 10
68 netic Circular Dichroism appears particularly interesting. 10

15 Author contributions

16 The manuscript was written through the contributions of all 15
17 authors. All authors have approved the final version of the 15
18 manuscript. 15

20 Conflicts of interest

21 There are no conflicts to declare. 20

25 Acknowledgements

26 We acknowledge the financial support by European COST 25
27 Action CA15128 MOLSPIN and the FET Open Femtotera- 25
28 byte project. The financial support by Italian MIUR for Progetto 25
29 Dipartimenti di Eccellenza 2018–2022 (ref. no. 30
30 B96C1700020008), for PRIN project Q-ChiSS (2017CR5WCH), 30
31 for Regione Toscana POR CreO FESR 2014–2020- SENSOR, and 30
32 Fondazione Ente Cassa di Risparmio di Firenze is also 30
33 acknowledged. 35

Notes and references

- 1 D. Gatteschi, R. Sessoli and J. Villain, *Molecular Nanomag-* 40
nets, Oxford University Press, 2006, vol. 54. 40
- 2 A. Candini, S. Klyatskaya, M. Ruben, W. Wernsdorfer and 40
M. Affronte, *Nano Lett.*, 2011, **11**, 2634–2639. 40
- 3 M. Urdampilleta, S. Klyatskaya, J.-P. Cleuziou, M. Ruben 40
and W. Wernsdorfer, *Nat. Mater.*, 2011, **10**, 502–506. 40
- 4 M. Ganzhorn, S. Klyatskaya, M. Ruben and W. Wernsdorfer, 45
Nat. Commun., 2016, **7**, 11443. 45
- 5 S. Thiele, F. Balestro, R. Ballou, S. Klyatskaya, M. Ruben and 45
W. Wernsdorfer, *Science*, 2014, **344**, 1135–1138. 45
- 6 L. Malavolti, V. Lanzilotto, S. Ninova, L. Poggini, I. Cimatti, 50
B. Cortigiani, L. Margheriti, D. Chiappe, E. Otero, 50
P. Sainctavit, F. Totti, A. Cornia, M. Mannini and 50
R. Sessoli, *Nano Lett.*, 2015, **15**, 535–541. 50
- 7 L. Margheriti, D. Chiappe, M. Mannini, P.-E. Car, 50
P. Sainctavit, M.-A. Arrio, F. B. de Mongeot, J. C. Cezar, 50
F. M. Piras, A. Magnani, E. Otero, A. Caneschi and 55
R. Sessoli, *Adv. Mater.*, 2010, **22**, 5488–5493. 55

- 1 8 M. Mannini, F. Pineider, C. Danieli, F. Totti, L. Sorace, P. Sainctavit, M.-A. Arrio, E. Otero, L. Joly, J. C. Cezar, A. Cornia and R. Sessoli, *Nature*, 2010, **468**, 417–421.
- 9 G. Serrano, L. Poggini, M. Briganti, A. L. Sorrentino, G. Cucinotta, L. Malavolti, B. Cortigiani, E. Otero, P. Sainctavit, S. Loth, F. Parenti, A.-L. L. Barra, A. Vindigni, A. Cornia, F. Totti, M. Mannini and R. Sessoli, *Nat. Mater.*, 2020, **19**, 546–551.
- 10 N. Ishikawa, M. Sugita, T. Ishikawa, S.-Y. Koshihara and Y. Kaizu, *J. Am. Chem. Soc.*, 2003, **125**, 8694–8695.
- 11 N. Ishikawa, *Polyhedron*, 2007, **26**, 2147–2153.
- 12 S. Takamatsu, T. Ishikawa, S. Koshihara and N. Ishikawa, *Inorg. Chem.*, 2007, **46**, 7250–7252.
- 13 L. Vitali, S. Fabris, A. M. Conte, S. Brink, M. Ruben, S. Baroni and K. Kern, *Nano Lett.*, 2008, **8**, 3364–3368.
- 14 N. Ishikawa, M. Sugita, N. Tanaka, T. Ishikawa, S. Y. Koshihara and Y. Kaizu, *Inorg. Chem.*, 2004, **43**, 5498–5500.
- 15 T. Komeda, H. Isshiki, J. Liu, Y.-F. Zhang, N. Lorente, K. Katoh, B. K. Breedlove and M. Yamashita, *Nat. Commun.*, 2011, **2**, 217.
- 16 T. Komeda, H. Isshiki, J. Liu, K. Katoh and M. Yamashita, *ACS Nano*, 2014, **8**, 4866–4875.
- 17 G. Serrano, E. Velez-Fort, I. Cimatti, B. Cortigiani, L. Malavolti, D. Betto, A. Ouerghi, N. B. Brookes, M. Mannini and R. Sessoli, *Nanoscale*, 2018, **10**, 2715–2720.
- 18 C. Wäckerlin, F. Donati, A. Singha, R. Baltic, S. Rusponi, K. Diller, F. Patthey, M. Pivetta, Y. Lan, S. Klyatskaya, M. Ruben, H. Brune and J. Dreiser, *Adv. Mater.*, 2016, **28**, 5195–5199.
- 19 S. Stepanow, J. Honolka, P. Gambardella, L. Vitali, N. Abdurakhmanova, T.-C. Tseng, S. Rauschenbach, S. L. Tait, V. Sessi, S. Klyatskaya, M. Ruben and K. Kern, *J. Am. Chem. Soc.*, 2010, **132**, 11900–11901.
- 20 S. Marocchi, A. Candini, D. Klar, W. Van den Heuvel, H. Huang, F. Troiani, V. Corradini, R. Biagi, V. De Renzi, S. Klyatskaya, K. Kummer, N. B. Brookes, M. Ruben, H. Wende, U. del Pennino, A. Soncini, M. Affronte and V. Bellini, *ACS Nano*, 2016, **10**, 9353–9360.
- 21 J.-P. Kappler, E. Otero, W. Li, L. Joly, G. Schmerber, B. Muller, F. Scheurer, F. Leduc, B. Gobaut, L. Poggini, G. Serrano, F. Choueikani, E. Lhotel, A. Cornia, R. Sessoli, M. Mannini, M.-A. Arrio, P. Sainctavit and P. Ohresser, *J. Synchrotron Radiat.*, 2018, **25**, 1727–1735.
- 22 M. Mannini, F. Bertani, C. Tudisco, L. Malavolti, L. Poggini, K. Misztal, D. Menozzi, A. Motta, E. Otero, P. Ohresser, P. Sainctavit, G. G. Condorelli, E. Dalcanale and R. Sessoli, *Nat. Commun.*, 2014, **5**, 4582.
- 23 M. Studniarek, C. Wäckerlin, A. Singha, R. Baltic, K. Diller, F. Donati, S. Rusponi, H. Brune, Y. Lan, S. Klyatskaya, M. Ruben, A. P. Seitsonen and J. Dreiser, *Adv. Sci.*, 2019, **6**, 1901736.
- 24 S. Baumann, W. Paul, T. Choi, C. P. Lutz, A. Ardavan and A. J. Heinrich, *Science*, 2015, **350**, 417–420.
- 25 F. Donati, S. Rusponi, S. Stepanow, C. Wäckerlin, A. Singha, L. Persichetti, R. Baltic, K. Diller, F. Patthey, E. Fernandes, J. Dreiser, Ž. Šljivančanin, K. Kummer, C. Nistor, P. Gambardella and H. Brune, *Science*, 2016, **352**, 318–321.
- 26 F. D. Natterer, K. Yang, W. Paul, P. Willke, T. Choi, T. Greber, A. J. Heinrich and C. P. Lutz, *Nature*, 2017, **543**, 226–228.
- 27 U. Diebold, *Surf. Sci. Rep.*, 2003, **48**, 53–229.
- 28 A. J. Haider, Z. N. Jameel and I. H. M. Al-Hussaini, *Energy Procedia*, 2019, **157**, 17–29.
- 29 D. O. Scanlon, C. W. Dunnill, J. Buckeridge, S. A. Shevlin, A. J. Logsdail, S. M. Woodley, C. R. A. Catlow, M. J. Powell, R. G. Palgrave, I. P. Parkin, G. W. Watson, T. W. Keal, P. Sherwood, A. Walsh and A. A. Sokol, *Nat. Mater.*, 2013, **12**, 798–801.
- 30 P. Palmgren, K. Nilson, S. Yu, F. Hennies, T. Angot, J.-M. Layet, G. Le Lay and M. Göthelid, *J. Phys. Chem. C*, 2008, **112**, 5972–5977.
- 31 P. Palmgren, B. R. Priya, N. P. P. Niraj and M. Göthelid, *Sol. Energy Mater. Sol. Cells*, 2006, **90**, 3602–3613.
- 32 S. Yu, S. Ahmadi, C. Sun, P. T. Z. Adibi, W. Chow, A. Pietzsch and M. Göthelid, *J. Chem. Phys.*, 2012, **136**, 154703.
- 33 S. Yu, S. Ahmadi, P. Palmgren, F. Hennies, M. Zuleta and M. Göthelid, *J. Phys. Chem. C*, 2009, **113**, 13765–13771.
- 34 K. Eguchi, Y. Takagi, T. Nakagawa and T. Yokoyama, *J. Phys. Chem. C*, 2013, **117**, 22843–22851.
- 35 L. Cao, Y. Wang, J. Zhong, Y. Han, W. Zhang, X. Yu, F. Xu, D.-C. Qi and A. T. S. Wee, *J. Phys. Chem. C*, 2011, **115**, 24880–24887.
- 36 V. Lanzilotto, G. Lovat, G. Fratesi, G. Bavdek, G. P. Brivio and L. Floreano, *J. Phys. Chem. Lett.*, 2015, **6**, 308–313.
- 37 S.-C. Li, L.-N. Chu, X.-Q. Gong and U. Diebold, *Science*, 2010, **328**, 882–884.
- 38 S. Yu, S. Ahmadi, C. Sun, P. Palmgren, F. Hennies, M. Zuleta and M. Göthelid, *J. Phys. Chem. C*, 2010, **114**, 2315–2320.
- 39 U. Diebold, J. Lehman, T. Mahmoud, M. Kuhn, G. Leonardelli, W. Hebenstreit, M. Schmid and P. Varga, *Surf. Sci.*, 1998, **411**, 137–153.
- 40 M. Li, W. Hebenstreit, U. Diebold, A. M. Tyryshkin, M. K. Bowman, G. G. Dunham and M. A. Henderson, *J. Phys. Chem. B*, 2000, **104**, 4944–4950.
- 41 U. Diebold and T. E. Madey, *Surf. Sci. Spectra*, 1996, **4**, 227–231.
- 42 J. T. Mayer, U. Diebold, T. E. Madey and E. Garfunkel, *J. Electron Spectrosc. Relat. Phenom.*, 1995, **73**, 1–11.
- 43 M. J. Jackman, A. G. Thomas and C. Muryn, *J. Phys. Chem. C*, 2015, **119**, 13682–13690.
- 44 W. S. Epling, C. H. F. Peden, M. A. Henderson and U. Diebold, *Surf. Sci.*, 1998, **412–413**, 333–343.
- 45 M. H. M. Ahmed, R. H. Temperton and J. N. O’Shea, *Surf. Interface Anal.*, 2020, 1–7.
- 46 W. S. Oh, C. Xu, D. Y. Kim and D. W. Goodman, *J. Vac. Sci. Technol., A*, 1997, **15**, 1710–1716.
- 47 M. Oku, K. Wagatsuma and S. Kohiki, *Phys. Chem. Chem. Phys.*, 1999, **1**, 5327–5331.
- 48 K. S. Kim and N. Winograd, *Chem. Phys. Lett.*, 1975, **31**, 312–317.
- 49 S. K. Sen, J. Riga and J. Verbist, *Chem. Phys. Lett.*, 1976, **39**, 560–564.

- 1 50 M. J. Jackman, A. G. Thomas and C. Muryn, *J. Phys. Chem. C*, 2015, **119**, 13682–13690.
- 51 A. Pedrini, L. Poggini, C. Tudisco, M. Torelli, A. E. Giuffrida, F. Bertani, I. Cimatti, E. Otero, P. Ohresser, P. Saintavit, 5 M. Suman, G. G. Condorelli, M. Mannini and E. Dalcanale, *Small*, 2018, **14**, 1702572.
- 52 B. Brena, Y. Luo, M. Nyberg, S. Carniato, K. Nilson, Y. Alfredsson, J. Åhlund, N. Mårtensson, H. Siegbahn and C. Puglia, *Phys. Rev. B: Condens. Matter Mater. Phys.*, 2004, 10 **70**, 1–6.
- 53 A. Cornia and M. Mannini, in *Molecular Nanomagnets and Related Phenomena*, ed. S. Gao, Springer Berlin Heidelberg, Berlin, Heidelberg, 2014, pp. 293–330.
- 54 R. Karstens, M. Glaser, A. Belser, D. Balle, M. Polek, 15 R. Ovsyannikov, E. Giangrisostomi, T. Chassé and H. Peisert, *Molecules*, 2019, **24**, 4579.
- 55 M. Batzill, K. Katsiev, D. J. Gaspar and U. Diebold, *Phys. Rev. B: Condens. Matter Mater. Phys.*, 2002, **66**, 235401.
- 56 R. A. Bennett, P. Stone, N. J. Price and M. Bowker, *Phys. Rev. Lett.*, 1999, **82**, 3831–3834. 20
- 57 G. Serrano, S. Wiespointner-Baumgarthuber, S. Tebi, S. Klyatskaya, M. Ruben, R. Koch and S. Müllegger, *J. Phys. Chem. C*, 2016, **120**, 13581–13586.
- 58 Y. Wang, Y. Ye and K. Wu, *J. Phys. Chem. B*, 2006, **110**, 25 17960–17965.
- 59 P.-E. Car, M. Perfetti, M. Mannini, A. Favre, A. Caneschi and R. Sessoli, *Chem. Commun.*, 2011, **47**, 3751.
- 60 N. Ishida and D. Fujita, *J. Phys. Chem. C*, 2012, **116**, 20300–20305.
- 61 J. Ø. Hansen, P. Huo, U. Martinez, E. Lira, Y. Y. Wei, R. Streber, E. Lægsgaard, B. Hammer, S. Wendt and F. Besenbacher, *Phys. Rev. Lett.*, 2011, **107**, 136102. 5
- 62 H. Hussain, G. Tocci, T. Woolcot, X. Torrelles, C. L. Pang, D. S. Humphrey, C. M. Yim, D. C. Grinter, G. Cabailh, O. Bikondoa, R. Lindsay, J. Zegenhagen, A. Michaelides and G. Thornton, *Nat. Mater.*, 2017, **16**, 461–466.
- 63 J. Balajka, M. A. Hines, W. J. I. DeBenedetti, M. Komora, J. Pavelec, M. Schmid and U. Diebold, *Science*, 2018, **361**, 786–789. 10
- 64 G. Serrano, B. Bonanni, T. Kosmala, M. D. Giovannantonio, U. Diebold, K. Wandelt and C. Goletti, *Beilstein J. Nanotechnol.*, 2015, **6**, 438. 15
- 65 G. Serrano, B. Bonanni, M. Di Giovannantonio, T. Kosmala, M. Schmid, U. Diebold, A. Di Carlo, J. Cheng, J. Vandevondele, K. Wandelt and C. Goletti, *Adv. Mater. Interfaces*, 2015, **2**, 1500246.
- 66 J. Lee, D. C. Sorescu, X. Deng and K. D. Jordan, *J. Phys. Chem. Lett.*, 2013, **4**, 53–57. 20
- 67 D. C. Hennessy, M. Pierce, K.-C. Chang, S. Takakusagi, H. You and K. Uosaki, *Electrochim. Acta*, 2008, **53**, 6173–6177.
- 68 J. A. J. Burgess, L. Malavolti, V. Lanzilotto, M. Mannini, S. Yan, S. Ninova, F. Totti, S. Rolf-Pissarczyk, A. Cornia, R. Sessoli and S. Loth, *Nat. Commun.*, 2015, **6**, 8216. 25

30

30

35

35

40

40

45

45

50

50

55

55